How Negatively Charged Proteins Adsorb to Negatively Charged Surfaces - a Molecular Dynamics Study of BSA Adsorption on Silica.

Karina Kubiak-Ossowska[a], B. Jachimska[b] and Paul A. Mulheran[a]*

[a]Department of Chemical and Process Engineering, University of Strathclyde, James Weir Building, 75 Montrose Street, Glasgow G1 1XJ, United Kingdom

[b]J. Harber Institute of Catalysis and Surface Chemistry, Polish Academy of Science (PAS), Niezapominajek 8, 30-239 Cracow, Poland

Corresponding Author

Karina Kubiak-Ossowska, tel. +44(0)141 548 3420; e-mail karina.kubiak@strath.ac.uk

Abstract

How proteins adsorb to inorganic material surfaces is critically important for the development of new biotechnologies, since the orientation and structure of the adsorbed proteins impacts their functionality. Whilst it is known that many negatively charged proteins readily adsorb to negatively charged oxide surfaces, a detailed understanding of how this process occurs is lacking. In this work we study the adsorption of BSA, an important transport protein that is negatively charged at physiological conditions, to a model silica surface that is also negatively charged. We use fully atomistic Molecular Dynamics to provide detailed understanding of the non-covalent interactions that bind the BSA to the silica surface. Our results provide new insight into the competing roles of long-range electrostatics and short-range forces, and the consequences this has for the orientation and structure of the adsorbed proteins.

Introduction

How does a negatively charged protein spontaneously attach itself to a negatively charged inorganic surface? In recent years there has been a lot of interest in the adsorption of proteins to inorganic materials, since this provides a means to developing new technologies such as drug delivery systems, diagnostics, and anti-bacterial coatings to name but a few.[1-4] In order to engineer new technologies, detailed understanding of the adsorption is required; the strength of the interactions dictate whether the adsorbed proteins can be released under certain environmental conditions, whilst the orientation and structure of the proteins dictates whether they can impart functionality to the material surface. Fully atomistic Molecular Dynamics (MD) simulation has a key role to play, providing detailed insight into the adsorption pathways and interactions that might otherwise be unobtainable. Simulations with negatively charged surfaces usually focus on proteins that have positive charge at physiological conditions, since electrostatics then guides the adsorption process in the 100ns timescale of a typical MD trajectory, whilst dictating protein orientation.[5-10]

The question of how negatively charged proteins adsorb to these negatively charged surfaces has not been addressed with the same atomistic detail. BSA is an important protein due to its ability to bind and transport drugs[11-14] and nanoparticles.[15] Experimentally, it is known that BSA will readily adsorb to silica substrates under physiological conditions where both protein and surface are negatively charged,[9,16-19] raising the question of the role of electrostatics in the process.[17,19,20] McUmber *et al.*[19] have shown that ionic screening of the charged surfaces is important for the adsorption rates, but the adsorption strength appears to be dictated by short-ranged non-covalent forces. However, whilst there have been a number of simulations of BSA

adsorption at different substrates,[21-23] an atomistic understanding of this phenomenon is lacking, and it is the purpose of this paper to provide this insight.

Computational Details

All simulations were performed with the NAMD 2.8[24] package using the CHARMM27 force-field, and analyzed using VMD.[25] 3V03[11] with all disulphide bridges kept was used as the starting BSA structure. We have prepared six simulation systems for various protein–surface orientations and after 100ns of the adsorption trajectory the most effective one was chosen to continue for a subsequent 100ns trajectory. For the chosen protein-surface orientation we obtained four independent, 200ns trajectories, however only one of them led to the BSA being adsorbed. It may reflect the long (for the MD time-scale) lag phase of BSA adsorption required for proper protein re-orientation with respect to the surface. Our set of various initial protein-surface orientations indicates that the adsorption pathway described here is likely to be the most relevant for this system.

The protein (-17e) was initially neutralized by NaCl at an ionic strength $I=5x10^{-2}M$, resulting in 38 Na^+ and 21 Cl^- ions. Then the SiO_2 surface slab (of 129Å x129Å; thickness 13Å) was neutralized by adding a further 429 Na+ ions. Note that in the experiments at pH 7.0, the silica has a negative zeta potential.[8,10,17-18,26-27] The silica surface model was constructed similarly to our previous work[10,28-30] using a $(10\bar{1})$ slab of α-crystabolite, nevertheless this time the slab has been cut from a bulk crystal in such a way as to leave siloxide groups ($\equiv SiO^-$) both at the top and bottom of the slab. The charge of the slab size used is -429e. The large size of the

periodic cell was forced by the BSA size which is ~80Å – 90Å in each direction; moreover the protein needs to have some gap (at least 20Å) between the surface and its image to avoid biased adsorption. Therefore the simulation box size was chosen to be 129Å x 129Å x 191Å. The primary simulation cell was filled by water (TIP3P model) and counter ions; the total number of atoms in the cell was ~240,000. We initially ran water and ion minimization followed by equilibration at constant temperature of 300K for 100ps, with an integration time step 1fs. In the next step we ran minimization of the entire system (water, ions and protein) for 10,000 steps and then equilibration at 300K for 6ns with integration time step 2fs. The production trajectories were 100ns or 200ns long, depending on the initial protein – surface orientation, as mentioned above. In all stages the surface atoms were kept immobile and we used the NVT ensemble with PBC and the PME method for calculating electrostatics, while the cutoff for VdW interactions was 12Å. To keep the temperature constant the Langevin thermostat (with damping parameter = 5 in NAMD units) was used. The PME grid size was 191x129x129 in x, y and z, respectively while the electrostatic frequency parameter was set up as 2 (NAMD units). To obtain the desired pressure of 1atm a flexible periodic cell was used. To reduce the computational time the all bonds and angles in the water molecules were constrained.

While we discuss the methods we would like to note that accelerated MD methods such as Steered MD (SMD) or Potential of Mean Force might provide additional data regarding the adsorption pathway. We believe that such simulations should start from a probable, unbiased adsorption state that is provided by MD simulation, since then we know that at least the system is in a locally stable configuration that might be difficult to sample form other configurations found by alternative means. We have previously demonstrated with a different protein-surface system that SMD might drive the adsorbed protein from one adsorbed configuration to another one,

which due to high energy barriers is not likely to be accessible in traditional MD simulation.[31] Such simulations are in progress for the BSA system.

Results and Discussion

Using fully atomistic MD simulation, we have studied the adsorption of BSA to a model silica substrate previously used with other protein adsorption simulations.[5-7,10,28,29,31,32] The BSA structure 3V03.pdb from the Protein Data Bank[11] is used in our simulations, which has 583 aminoacids (note the first two residues, namely Asp1 and Thr2, both uncharged and hydrophilic are missing, but these do not affect the protein's overall structure or properties). The protein is divided into three domains, each of which has two sub-domains,[11] as illustrated in Fig. 1(A). The protein comprises 29 alpha-helices and its tertiary structure is maintained through a network of seventeen disulphide bridges. The overall charge of the protein at pH7 is -17e, however there are numerous positively charged Arg and Lys as well as negatively charged Asp and Glu residues in the protein, so that its surface charge distribution is inhomogeneous as illustrated in Fig. 1(B). The subdomains also have different total charges as summarized in Table 1.

From Table 1, we see that the domain III is positively charged in comparison to the other two domains. This yields a significant dipole moment of 650D (as measured using the VMD software[25]) pointing from subdomain IIA towards subdomain IIIB as indicated in Fig. 1 by the yellow needle. This suggests that the protein will prefer to adsorb to the negatively charged silica surface using domain III.

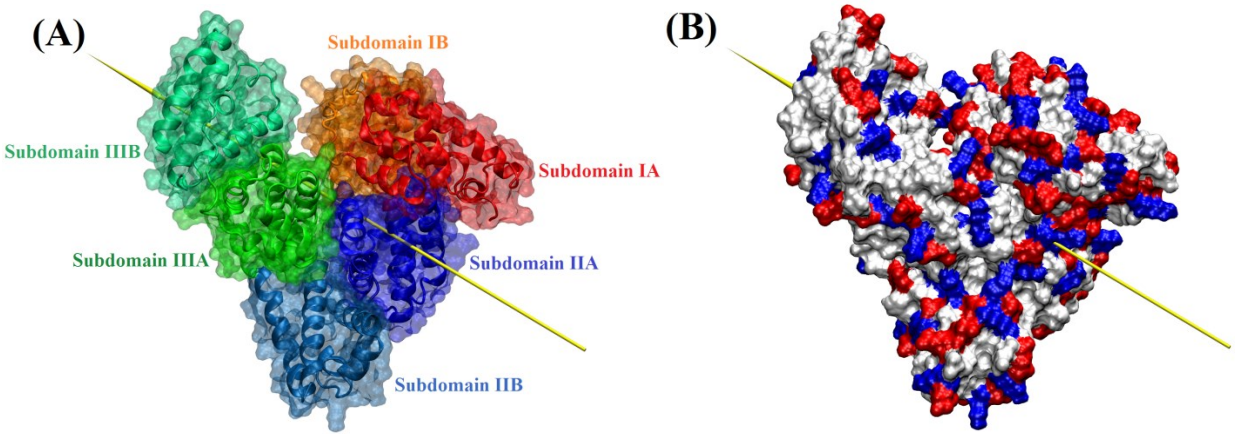

Figure1. BSA structure (A), and charge distribution (B) on the protein surface. In (A) the protein 'ghost' surface is shown alongside the secondary structure elements displayed as 'cartoon'.[25] Domain I is indicated by red-related colors (IA – red, IB – orange), domain II by blue-related colors (IIA – blue, IIB – light blue) and domain II by green-related colors (IIIA – green, IIIB – lime). The color scheme used is similar to those introduced by Majorek *et al*.[11] All subdomains are annotated and the yellow arrow indicates the protein dipole moment as defined in VMD.[25] In (B) the protein surface is shown as 'solid'[25] and colored by residue charge (positive is blue, negative is red, and neutral is white).

Table 1. BSA charged residues within subdomains, domains and the full protein. Second column lists number of residues per structure, while the following lists the number of charged, positive and negative residues per structure. The last column lists the total charge.

Structure	Number of				Total charge
	Residues	Charged	Positive	Negative	
IA	105	32	11	21	-10
IB	86	27	13	14	-1
I	191	59	24	35	-11
IIA	103	37	19	18	+1
IIB	88	28	10	18	-8
II	191	65	29	36	-7
IIIA	113	29	16	13	+3
IIIB	86	26	12	14	-2
III	199	55	28	27	+1
BSA	**581**	**179**	**81**	**98**	**-17**

In our simulation, we use a silica slab model that exposes negatively charged and under-coordinated oxygen species at its surface. The surface has a net negative charge, which is balanced by the addition of positive Na^+ ions (429 in the case studied here) in the water above it. In addition, we also neutralize the charge of the BSA, and further add Na^+ and Cl^- ions to create an ionic strength $I=5x10^{-2}M$ in the water. Due to the fact that the surface charge must be neutralised in the system to represent the electrostatic environment above the surface, the bulk solution ionic strength is not expected to have a noticeable impact on the adsorption process studied. Moreover, our previous studies indicate that a higher ionic strength mainly slows down

the adsorption without greatly influencing its mechanism, protein orientation on the surface or list of important interacting residues.[30] During the simulations, the ionic distribution rapidly equilibrates and the charged surface is screened by the Na^+ ions, so that far above the surface there is no time-averaged electric field. This means that the BSA is free to diffuse and rotate in the water, and indeed most of our simulation trajectories just display this behavior without any adsorption occurring within a reasonable simulation timescale of ~100ns – 200ns; we will not discuss these trajectories further in this paper. Close to the surface, within the Na^+ diffuse layer screening the surface, there is a persistent electric field that can steer the adsorption of the protein. The extent of this layer in our simulations is apparent in Figure 2, where we see that it is much smaller that the BSA subdomains. This suggests that with the correct orientation, positive regions of the protein can interact with the surface whilst negative regions can remain above the screening layer.

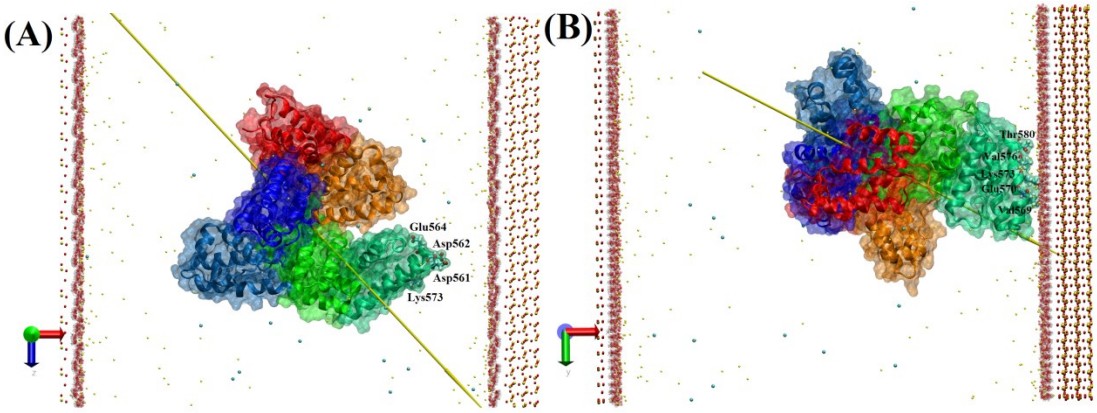

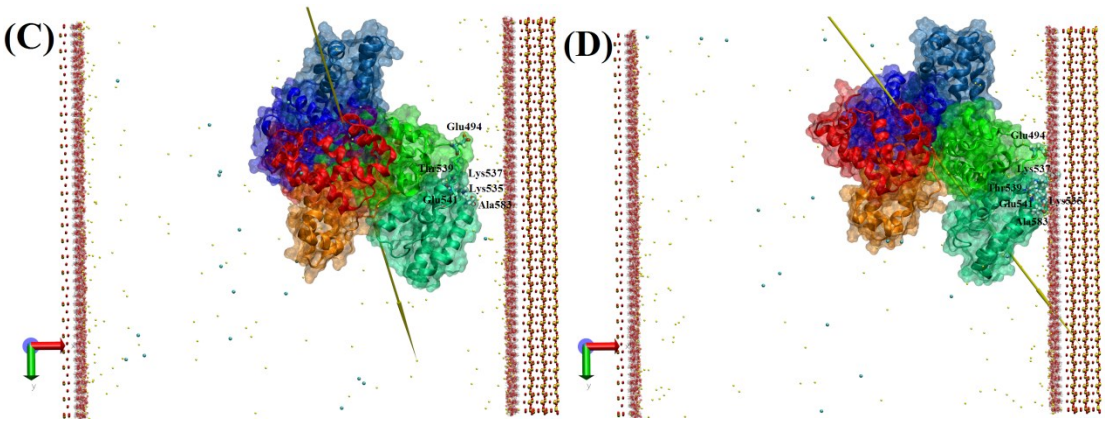

Figure 2. Snapshots illustrating the adsorption trajectory: (A) starting configuration; (B) at 93ns; (C) at 133ns; (D) at 186ns. The protein colour scheme follows that of Fig. 1. The key residues are shown by the licorice representation as defined in VMD[25] colored by name (oxygen-red, carbon-cyan, nitrogen-blue, hydrogen-white) and annotated. The oxygen of the silica surface is red and the silicon yellow. The water has red oxygen and white hydrogen, with yellow sodium and blue chlorine ions. For clarity, only the water in the surface layers are shown.

In Fig. 2(A) we show a snapshot of the successful adsorption simulation at the start of the trajectory, following the equilibration protocol described below in the methods section. The minimum distance between any atom of the BSA and any atom of the surface is 20Å, and the corresponding distance is 35Å to the image surface that is present due to the periodic boundary conditions employed in the simulations. The BSA is oriented so that subdomain IIIB is facing the surface, since it is only in this orientation that we find a successful adsorption event within reasonable trajectory duration. No additional constraints are used in the simulations, so the protein is free to rotate and diffuse, coming to interact with the surface in an unbiased way.

Furthermore, the water and ions are also free to diffuse (the surface atoms are held fixed in the simulation), creating a fluctuating electric field in the vicinity of the silica and protein surfaces.

In Figure 3 we show the Centre-of-Mass (CoM) movement of the BSA during the adsorption simulation. Figure 3(A) gives a plan view of the CoM motion across the surface, with different sections of the trajectory labeled for convenience. The corresponding sections are also shown in Figure 3(B) for the distances between the CoM and the uppermost surface atoms. Section A of the trajectory is the initial 40ns of the trajectory, where the BSA diffuses freely in the water above the surface. During section B for the following 40ns, the protein moves steadily towards the surface, indicating that there is a long-range attraction to the surface as the residues in subdomain IIIB diffuse close enough to the surface to feel the fluctuating electric field within the ionic screening layer of the surface. In section C of the trajectory there is a weak binding to the surface (CoM distance to the surface ~52Å) that only lasts about 20ns, following which the protein loses contact with the surface and the protein again diffuses across the surface in section D. In section E, from 150ns – 180ns, the protein CoM moves even closer to the surface, and finally in section F we find a long-lived adsorbed state where the CoM fluctuates only by about +/- 3Å across the substrate due to the flexing of the protein about its anchoring site (CoM distance to the surface ~42Å).

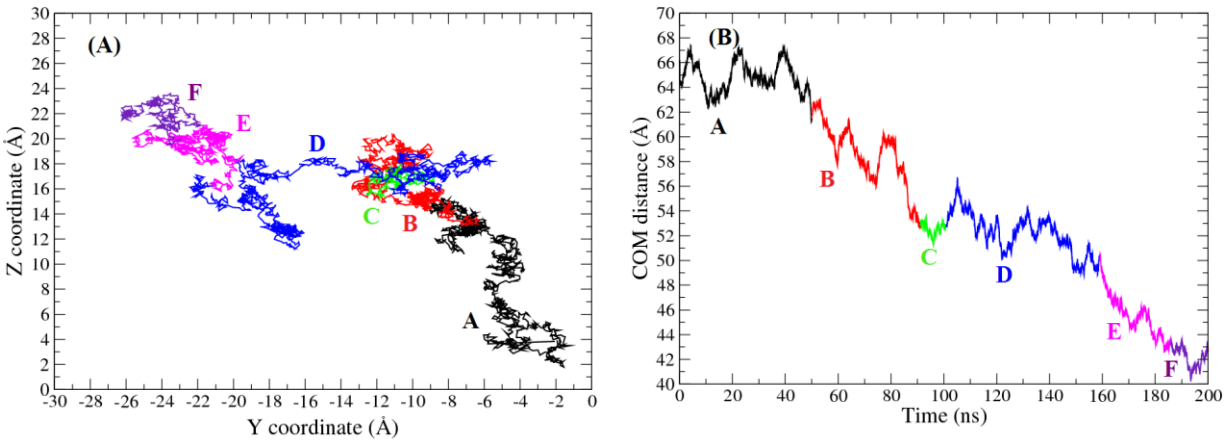

Figure 3. The CoM movement of the protein during the adsorption simulation: (a) plan view of the surface; (b) side view showing separation from the surface plane. The different stages of the adsorption trajectory are labeled.

During the initial movement towards the surface, section B of the trajectory in Figure 3, the positively charged Lys573 residue is extended from the protein surface and helps steer it towards the surface; the protein slowly rotates during its movement towards the surface. As shown in Figure 2(B), during the temporary interaction stage of section C, Lys573 is one of the residues at the protein surface interacting with the silica surface. Of the other residues left exposed towards the silica surface, Glu570 is negatively charged, which might help account for the temporary nature of this state. Moreover, the CoM distance from the surface in section C is 52Å, compared to 42Å in section F, which indicates that section C is rather temporary. The time spent in this section is short (20ns), and the protein does not return to this conformation within the subsequent 200ns trajectory (data not shown). In Figure 2(C), we show the configuration in section D of the trajectory when the protein starts to diffuse again above the surface. The protein is able also to rotate further, now exposing Lys537 (not Lys573) to the silica surface as it

approaches in section E of the trajectory. This time, the positive residue remains extended as it approaches and interacts directly with the silica oxygen atoms. The final adsorbed state of section F is shown in Figure 2(D), where we find that another positively charged residue Lys535 is also at the protein-silica interface, albeit with a layer of water between itself and the silica.

In the final adsorption state, Figure 2(D) also shows that other residues are at the protein-silica interface as well as the positive Lys537 and Lys535, namely the negatively charged Glu494, Glu541 and the negative terminus Ala583, as well as the neutral Thr539. Additionally Thr495, Gln542 and Thr580 (not shown on the figure to keep it clear) seem to be important for stabilizing the BSA adsorption by interacting with the water and/or ion layers. However, note that negative residues tend to be further from the interface, suggesting that they are better screened from the silica by the Na^+ ions that are attracted to them.

In Figure 4 we show in more detail what is happening at the silica surface. The water adopts a layered structure at the ionic surface, as reported elsewhere,[5,30] with slower dynamics than in the bulk solution. The Na^+ ions are incorporated into this structure, being more prominent in the outer layer than the inner one. During the temporary interaction (section C of the trajectory) Lys573 interacts only with the outer water layer. However, in the final adsorption state (section F of the trajectory) there is a strong interaction between Lys537 and the silica surface. Fig. 4 shows that the Lys537 penetrates both water layers, displacing two water molecules from both the inner and outer layers. Its anchoring role is aided by its approach to the surface during section E of the trajectory, where the positive side chain is extended in the electric field and able to digitate effectively into the water layers, so that its charged end group can interact with the negative oxygen of the surface.

The adsorption state appears to be stable, and a subsequent 200ns trajectory extension to section F shows that the adsorbed protein remains adsorbed, although it is still able to diffuse on the surface. In the adsorbed configuration, there are at least 6 hydrogen bonds (temporally even ~10 can be established) between the BSA residues and the outer water layer, plus 2 between the Lys537 and the inner water layer at the silica surface. According to the conclusions of Kurrat et al, this is sufficient for strong protein adsorption;[33] a similar conclusion has been made for HEWL adsorption on a model charged surface.[31] Nevertheless, fluctuations of individual residue side chains can still occur whilst the BSA remains adsorbed to the surface. In particular, Lys537 side chain desorption allows the BSA to find the most favorable orientation on the surface or, as we observe during the additional 200ns trajectory, to diffuse just above the structured water layers. This diffusion terminates when the Lys537 side-chain returns to its digitated orientation, re-establishing direct contact with the surface. It is worth noting that in the trajectory section C only one hydrogen bond (Lys573 – inner water layer) is created, again suggesting that this section represents a transient adsorption state.

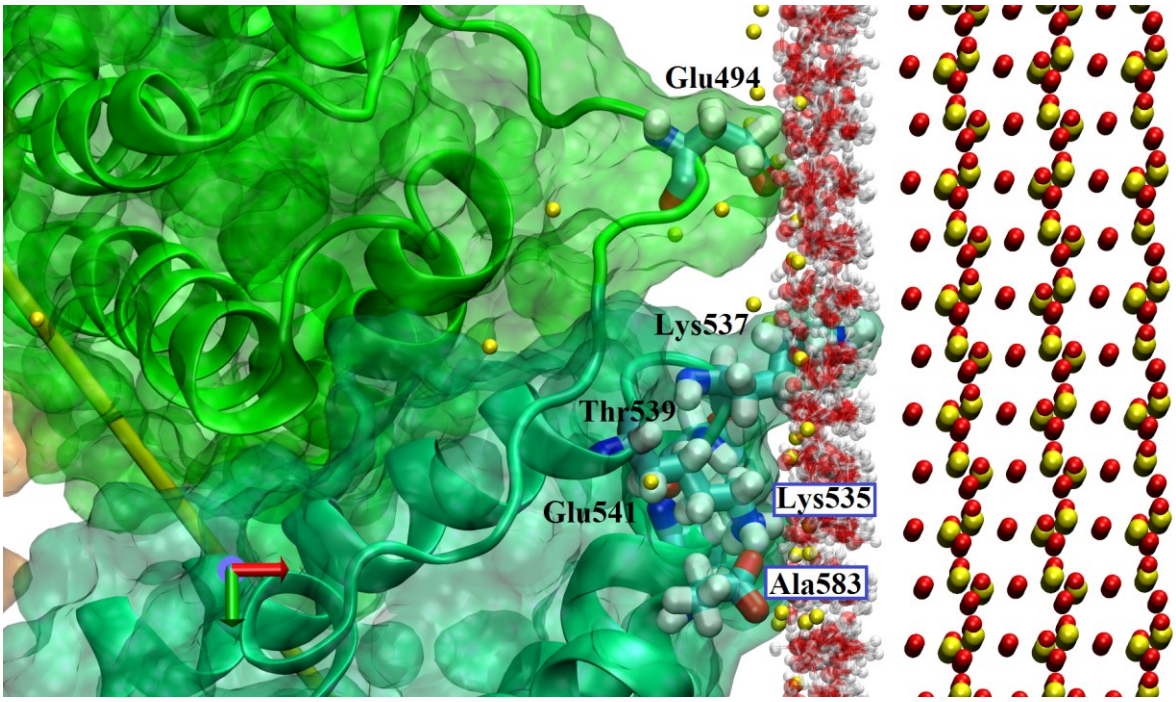

Figure 4. Close-up view of the adsorption state. The color scheme follows that of Fig. 2.

Conclusions

We can summarize the adsorption sequence of the BSA to the model silica surface that we have observed here as follows:

1. Above the surface and its ionic screening layer, the protein diffuses freely and can rotate to present its IIIB sub-domain towards the surface.

2. If the protein approaches the surface in this orientation, the positively charged residues at the protein surface feel the fluctuating electric field of the surface as the screening ions undergo thermal diffusion.

3. Lys residues extend their long side chains towards the surface, driven by their positively charged end groups.

4. The protein is attracted to the surface, since the negative subdomains remain above the screening layer.

5. If the orientation of the protein is only partially correct, the interactions are weak and the protein can desorb.

6. With correct orientation, the extended Lys side chains can penetrate both water layers above the surface to create strong anchors to the surface. The protein now is in a stable adsorbed state.

This sequence shows the dominant role that electrostatics plays in the adsorption process. While we have found only one successful adsorption trajectory in this study, and therefore might be missing alterative adsorption pathways, we note that our observations have many similarities to our earlier conclusions about the adsorption pathway for positively charged proteins to a negative oxide surface,[10,16,29,34] with the new insight here being the key role that the screening ions play in enabling the adsorption. The negatively charged domains of the protein are kept away from the surface and screened from its repulsive influence by the presence of the counter-ions. That electrostatics plays such an important role, particularly in the initial attraction and orientation of the protein, agrees well recent experimental results of McUmber *et al*.,[19] where it is reported that adsorption rate depends on pH and ionic strength. Interestingly, in that study surface residence times for the adsorbed BSA did not show similar dependencies on pH and ionic strength, so that the strength of the adsorption is dictated by molecular-scale details of the bonding interactions at the surface, just as we have found here in our simulations.

While we have studied one system here, namely BSA at pH7 adsorbing onto a model negatively charged silica surface, we expect that the adsorption sequence will be found to be generally applicable to proteins with similar (or even better) conformational stability to BSA in future work. This is because electrostatics and the screening due to counter ions play such an important role in the adsorption pathway of proteins, and particularly so for negatively charged proteins to negatively charged surfaces.

Acknowledgement

This work was supported by Grant NCN OPUS4 2012/07/B/ST5/00767. The simulations were performed on the EPSRC funded ARCHIE-WeSt High Performance Computer (www.archie-west.ac.uk); EPSRC grant no. EP/K000586/1.

References

(1) Thobhani, S.; Attree, S.; Boyd, R.; Kumarswami, N.; Noble, J.; Szymanski, M.; Porter, R. A. Bioconjugation and characterisation of gold colloid-labelled proteins. *J. Immunol. Methods* **2010**, *356*, 60-69.

(2) Goli, K. K.; Gera, N.; Liu, X.; Rao, B. M.; Rojas, O. J.; Genzer, J. Generation and Properties of Antibacterial Coatings Based on Electrostatic Attachment of Silver Nanoparticles to Protein-Coated Polypropylene Fibers. *ACS Appl. Mater. Interfaces* **2013**, *5,* 5298–5306.

(3) Zhang, H.; Chiao, M. Anti-fouling Coatings of Poly(dimethylsiloxane) Devices for Biological and Biomedical Applications. *J. Med. Biol. Eng.* **2015**, *35*, 143-155.

(4) Schottler, S.; Becker, G.; Winzen, S.; Steinbach, T.; Mohr, K.; Landfester, K.; Mailander, V.; Wurm, F. R. Protein adsorption is required for stealth effect of poly(ethylene glycol)- and poly(phosphoester)-coated nanocarriers. *Nature Nanotech.* **2016**, *11*, 372-377.

(5) Kubiak, K.; Mulheran, P. A. Molecular Dynamics Simulations of Hen Egg White Lysozyme Adsorption at a Charged Solid Surface. J. *Phys. Chem. B* **2009**, *113*, 12189-121200.

(6) Kubiak-Ossowska, K.; Mulheran, P. A. What Governs Protein Adsorption and Immobilization at a Charged Solid Surface? *Langmuir* **2010**, *26*, 7690-7694.

(7) Kubiak-Ossowska, K.; Mulheran, P. A. Mechanism of Hen Egg White Lysozyme Adsorption on a Charged Solid Surface. *Langmuir* **2011**, *26*, 15954-15965.

(8) Mathé, Ch.; Devineau, S.; Aude, J-Ch.; Lagniel, G.; Chédin, S.; Legros, V.; Mathon, M.-H.; Renault, J.-P.; Pin, S.; Boulard, Y et al. Structural Determinants for Protein adsorption/non-adsorption to Silica Surface. *PLOS ONE* **2013**, *8*, e81346.

(9) Benavidez, T. E.; Torrente, D.; Marucho M.; Garcia, C. D. Adsorption of Soft and Hard Proteins onto OTCEs under the Influence of an External Electric Field. *Langmuir*, **2015**, *31*, 2455-2462.

(10) Kubiak-Ossowska, K.; Cwieka, M.; Kaczynska, A.; Jachimska, B.; Mulheran, P. A. Lysozyme adsorption at a silica surface using simulation and experiment: effects of pH on protein layer structure. *PCCP* **2015**, *17*, 24070-24077.

(11) Majorek, K. A.; Porebski, P. J.; Dayal, A.; Zimmerman, M. D.; Jablonska, K.; Stewart, A. J.; Chruszcz, M.; Minor, W. Structural and immunologic characterization of bovine, horse, and rabbit serum albumins. *Mol. Immunol.* **2012**, *52*, 174–182.

(12) Bujacz, A.; Zielinski, K.; Sekula, B. Structural studies of bovine, equine, and leporine serum albumin complexes with naproxen. *Prot. Struct. Funct. Bioinformatics* **2014**, *82*, 2199-2208.

(13) Rub, M. A.; Khan, J. M.; Asiri, A. M.; Khan R. H.; Un-Din, K. Study on the interaction between amphiphilic drug and bovine serum albumin: A thermodynamic and spectroscopic description. *J. Luminescence* **2014**, *155,* 39-46.

(14) Abdelhameed, A. S. Insight into the Interaction between the HIV-1 Integrase Inhibitor Elvitegravir and Bovine Serum Albumin: A Spectroscopic Study. *J. Spectroscopy* **2015**, 435674.

(15) Russell, B. A.; Kubiak-Ossowska, K.; Mulheran, P. A.; Birch, D. J. S.; Chen, Y. Locating the nucleation sites for protein encapsulated gold nanoclusters: a molecular dynamics and fluorescence study. *PCCP* **2015**, *17*, 21935-21941.

(16) Jachimska, B.; Pajor, A.; Physico-Chemical Characterization of Bovine Serum Albumin in solution and as deposited on surfaces. *Bioelectrochemistry* **2012**, *87*, 136-146.

(17) Jachimska, B.; Tokarczyk, K.; Łapczyńska, M.; Puciul-Malinowska, A.; Zapotoczny, Sz. Structure of bovine serum albumin adsorbed on silica investigated by quartz crystal microbalance. *Col. Surf. A* **2016**, *489*, 163-172.

(18) Nooney, R. I.; White, A.; O'Mahony, Ch.; O'Connell, C.; Kelleher, A. M.; Daniels, S.; McDonagh, C. Investigating the colloidal stability of fluorescent silica nanoparticles under isotonic conditions for biomedical applications. *J. Col. Int. Sci.* **2015**, *456*, 50-58.

(19) McUmber, A. C.; Randolph, T. W.; Schwartz, D. K. Electrostatic Interactions Influence Protein Adsorption (but Not Desorption) at the Silica–Aqueous Interface. *Phys. Chem. Lett.* **2015**, *6*, 2583-2587.

(20) Li, W.; Li, S. A study on the adsorption of bovine serum albumin onto electrostatic microspheres: Role of surface groups. *Coll. Surf. A* **2007**, *295*, 159-164.

(21) Mucksch, Ch.; Urbassek, H. M. Molecular Dynamics Simulation of Free and Forced BSA Adsorption on a Hydrophobic Graphite Surface. *Langmuir* **2011**, *27*, 12938–12943.

(22) Delgado-Magnero, K. H.; Valiente, P. A.; Ruiz-Pena, M.; Perez-Gramatges, A.; Pons, T. Unraveling the binding mechanism of polyoxyethylene sorbitan esters with bovine serum albumin: A novel theoretical model based on molecular dynamic simulations. *Coll. Surf. Biointerfaces* **2015**, *116*, 720-726.

(23) Gu, Z.; Zaixing, Y.; Chong, Y.; Ge, C.; Weber, J. K.; Bell, D. R.; Zhou, R. Surface Curvature Relation to Protein Adsorption for Carbon-based Nanomaterials. *Scientific Reports* **2015**, *5*, 10886 .

(24) Phillips, J. C.; Braun, R.; Wang, W.; Gumbart, J.; Tajkhorshid, E.; Villa, E.; Chipot, Ch.; Skeel, R. D.; Kale, L.; Schulten, K. Scalable Molecular Dynamics with NAMD. *J. Comput. Chem.* **2005**, *26*, 1781–1802.

(25) Humphrey, W.; Dalke, A.; Schulten, K. VMD: visual molecular dynamics. *J. Mol. Graphics* **1996**, *14*, 33–38.

(26) Rezwan, K.; Meier, L. P.; Gauckler, L. J. Lysozyme and bovine serum albumin adsorption on uncoated silica and AlOOH-coated silica particles: the influence of positively and negatively charged oxide surface coatings. *Biomaterials* **2005**, *26*, 4351-4357.

(27) Wisniewska, M.; Szewczuk-Karpisz, K.; Sternik, D. Adsorption and thermal properties of the bovine serum albumin–silicon dioxide system. *J. Therm. Anal. Calorim*. **2015**, *120*, 1355–1364.

(28) Kubiak-Ossowska, K.; Burley, G.; Patwardhan, S. V.; Mulheran, P. A. Spontaneous Membrane-Translocating Peptide Adsorption at Silica Surfaces: A Molecular Dynamics Study. *J. Phys. Chem. B* **2013**, *117*, 14666-14675.

(29) Kubiak-Ossowska, K.; Mulheran, P. A.; Nowak, W. Fibronectin Module $FN^{III}9$ Adsorption at Contrasting Solid Model Surfaces Studied by Atomistic Molecular Dynamics. *J. Phys. Chem. B* **2014**, *118*, 9900–9908.

(30) Mulheran, P. A.; Connell, D. J.; Kubiak-Ossowska, K. Steering Protein Adsorption at Charged Surfaces: Electric Fields and Ionic Screening. *RSC Adv.* **2016**, *6*, 73709-73716.

(31) Kubiak-Ossowska, K.; Mulheran, P. A. Protein Diffusion and Long-Term Adsorption States at Charged Solid Surfaces. *Langmuir* **2012**, *28*, 15577–15585.

(32) Kubiak-Ossowska, K.; Muheran, P. A. Multiprotein Interactions during Surface Adsorption: a Molecular Dynamics Study of Lysozyme Aggregation at a Charged Solid Surface. *J. Phys. Chem. B* **2011**, *115*, 8891-8900.

(33) Kurrat, R.; Prenosil, J. E.; Ramsden, J. J. Kinetics of Human and Bovine Serum Albumin Adsorption at Silica-Titania Surfaces. *J. Col. Int. Sci.* **1997**, *185*, 1-8.

(34) Jachimska, B.; Kozlowska, A.; Pajor-Swierzy, A. Protonation of Lysozyme and Its consequences for the Adsorption onto a Mica Surface, *Langmuir*, **2012**, *28*, 11502-11510.

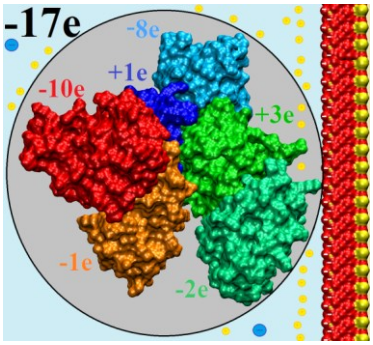
-17e
-8e
+1e
-10e
+3e
-1e
-2e